# INTERNATIONAL SOCIETY FOR SOIL MECHANICS AND GEOTECHNICAL ENGINEERING



This paper was downloaded from the Online Library of the International Society for Soil Mechanics and Geotechnical Engineering (ISSMGE). The library is available here:

## https://www.issmge.org/publications/online-library

This is an open-access database that archives thousands of papers published under the Auspices of the ISSMGE and maintained by the Innovation and Development Committee of ISSMGE.

The paper was published in the proceedings of the 20<sup>th</sup> International Conference on Soil Mechanics and Geotechnical Engineering and was edited by Mizanur Rahman and Mark Jaksa. The conference was held from May 1<sup>st</sup> to May 5<sup>th</sup> 2022 in Sydney, Australia.

# Energy transfer characteristics of standard penetration test using high-speed camera and instrumentations

Caractéristiques de transfert d'énergie du test de pénétration standard utilisant une caméra haute vitesse et des instrumentation

Eric H. Y. Sze, Philip W. K. Chung & Eugene K. L. Wong

Civil Engineering and Development Department, The Government of Hong Kong SAR, Hong Kong SAR, erichysze@cedd.gov.hk

Louis N. Y. Wong

Department of Earth Sciences, The University of Hong Kong, Hong Kong SAR

ABSTRACT: Standard Penetration Test (SPT) N-values require corrections for engineering application. Amongst others, the correction for energy efficiency of the SPT equipment is well-known for its high uncertainty. With a view to establishing the energy correction factor applicable to the ground investigation practice in Hong Kong, over 4,000 energy measurement data have been collected in various sites with different ground conditions and site exploration equipment. The results aim to provide technical basis for rationalizing the local practice of using SPT in respect of energy correction. In this paper, the results obtained for an automatic trip hammer at a reclamation site involving a very deep borehole (> 60 m) are presented. In particular, the entire energy transfer process is carefully studied by (1) capturing the hammer impact process using a modern high-speed camera, and (2) monitoring the post-impact stress wave travel along the drill rod assembly using strain gauges and accelerometers. Observations pertaining to the stress wave propagation characteristics have been made for soils with contrasting penetration resistance. For this site, the results reveal that the average stress wave energy that is effectively transmitted into the drill rod ranges from 60 to 70% of the theoretical impact energy, in which a notable amount of energy loss is found to take place before the hammer-anvil contact.

RÉSUMÉ : Le nombre de coups N (résistance à la pénétration) du test de pénétration standard (SPT) nécessitent des corrections pour l'application d'ingénierie. Entre autres, la correction de l'efficacité énergétique de l'équipement SPT est bien connue pour sa grande incertitude. En vue d'établir le facteur de correction énergétique applicable à la pratique d'investigation au sol à Hong Kong, plus de 4 000 données de mesure d'énergie ont été collectées dans divers sites avec des conditions de terrain et des équipements d'exploration de site différents. Les résultats visent à fournir une base technique pour rationaliser la pratique locale d'utilisation de SPT en matière de correction d'énergie. Dans cet article, les résultats obtenus pour un marteau-piqueur automatique sur un site de remise en état impliquant un forage très profond (> 60 m) sont présentés. En particulier, l'ensemble du processus de transfert d'énergie est soigneusement étudié en (1) capturant le processus d'impact du marteau à l'aide d'une caméra moderne à grande vitesse, et (2) en surveillant le trajet de l'onde de contrainte après impact le long de l'ensemble de tige de forage à l'aide de jauges de contrainte et d'accéléromètres . Des observations relatives aux caractéristiques de propagation des ondes de contrainte ont été faites pour des sols à résistance à la pénétration contrastée. Pour ce site, les résultats révèlent que l'énergie moyenne des ondes de contrainte qui est effectivement transmise dans la tige de forage varie de 60 à 70% de l'énergie d'impact théorique, dans laquelle une quantité notable de perte d'énergie se produit avant le marteau. contact d'enclume.

KEYWORDS: ground investigation, standard penetration test, energy efficiency, high-speed camera, wave propagation

#### 1 INTRODUCTION

The Standard Penetration Test (SPT) is an in-situ test commonly used for the characterisation of ground conditions. The test results, expressed as an N-value (defined as the total hammer blow counts for a sampler to penetrate over 300 mm into the ground), has been correlated with a number of geotechnical design parameters for engineering applications, e.g. estimation of soil parameters (Stroud 1988), design of foundation (Terzaghi & Peck 1967) and assessment of liquefaction potential (Andrus & Stokoe 2000). Although the definition of the N-value is standardised, there remain many non-standard variables in the SPT equipment and its operation that could affect the test results. Seed et al (1985) and Skempton (1986) discussed various pertinent factors and proposed corrections to the measured N-value. Amongst others, the correction of energy efficiency of the SPT equipment is known for its high uncertainty. The standard practice for energy correction is to adjust the N-value to a reference energy transfer ratio of 60%, denoted as  $N_{60}$ , following Eq. 1 (ISO 2005).

$$N_{60} = \frac{ETR}{60} \times N \tag{1}$$

where ETR is the energy transfer ratio of a specific SPT equipment, which is determined from in-situ instrumentation following standard procedures (ASTM 2016). In essence, ETR is a measure of the SPT system efficiency in delivering the hammer driving energy into the drill rod assembly. Batilas *et al* (2016) provided a comprehensive summary of ETR reported in the literature and indicated that its values could vary by a factor of two even for the same type of hammer and release technique. It is, therefore, important to establish the ETR specific to the local SPT practice.

In Hong Kong, the representative ETR of SPT is not well-established. Only limited studies have been undertaken. Kwong (1997) conducted in-situ measurements of the energy efficiency of an automatic trip hammer using a pile driving analyser and recorded ETR ranging from 29% to 43%, which were much lower than the typical values reported in the literature. Yang (2006) and Yang *et al* (2012) presented the development of an automatic monitoring system for SPT and calculated a mean ETR of about 56% using the Force Squared-Time (F<sup>2</sup>) method

(Schmertmann & Palacios 1979), which was later found to be erroneous compared with the state-of-the-art Force Velocity (FV) method (Howie *et al* 2003). The lack of reliable local data thus calls for a more comprehensive investigation on the SPT energy efficiency pertaining to the local ground investigation practice in Hong Kong.

Since 2018, the Geotechnical Engineering Office of The Government of Hong Kong SAR has launched a territory-wide study to systematically evaluate the energy efficiency of the SPT equipment commonly used in Hong Kong with a view to rationalising the SPT standard in respect of energy correction. So far, over 4,000 energy data have been collected in various sites covering different ground conditions, site exploration equipment and operation personnel. This paper provides a focused report on the results for a reclamation site involving a (> 60 m) covering soils with contrasting deen borehole penetration resistance. The hammer impact process was recorded using a modern high-speed camera whilst the stress wave propagation along the drill rod assembly was monitored using instrumentations. Apart from evaluating the ETR, the results shed light on the effect of soil penetration resistance on the stress wave propagation characteristics and quantify the energy loss of the automatic trip hammer release process.

#### 2 SPT EQUIPMENT AND MONITORING SYSTEM

Figure 1 shows the SPT equipment and the monitoring system adopted in this study, which are briefly described as follows.

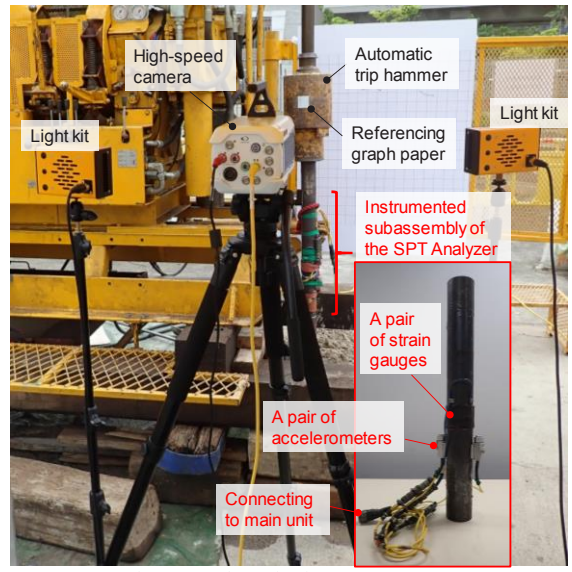


Figure 1. SPT equipment and monitoring system.

## 2.1 SPT equipment

In Hong Kong, the automatic trip hammer is the only accepted hammer and release system for SPT. Details regarding the testing procedure and the associated apparatus follow HKSARG (2006). Due to the tight control of the local ground investigation works, the variation of the SPT practice in terms of hardware usage is not large. The difference mainly falls on the different site exploration equipment used (e.g. drill rig) and the workmanship of different ground investigation contractors.

## 2.2 High-speed camera

A high-speed camera, *Phantom v711*, with a maximum frame rate of 7,530 frames per second (fps) at a full resolution of 1280  $\times$  800, was used. In this study, a frame rate up to 4,000 fps was used to record the hammer impact process. The camera was

placed at about 1.5 m away from the SPT equipment, where the hammer-anvil impact took place, with lighting provided by two external light sources. A graph paper was placed on the hammer to facilitate subsequent image analysis. To track the hammer displacement manually, the positions of a reference point on the graph paper were tracked using a two-dimensional motion analysis software *Tracker v4.11.0* (Brown, 2009). Particle image velocimetry (PIV) using the program PIVlab (Thielicke & Stamhuis 2014) has also been employed to analyse the motion during the hammer-anvil interaction.

#### 2.3 Instrumentation monitoring

The commercial product, SPT Analyzer (PDI, 2005), was used to monitor the stress wave propagation and measure the energy transfer efficiency of the SPT. It comprises a main unit for data acquisition, control and display of input and output data as well as a rod section of an instrumented subassembly mounted with a pair of strain gauges (for force measurement) and a pair of piezoresistive accelerometers (for velocity measurement). Each pair of instruments is symmetrically arranged to avoid any bending effects. The instrumented rod is installed between the hammer-anvil assembly and the drill rod assembly. Upon each hammer blow, the SPT Analyzer would be triggered to measure the time histories of the force and velocity of the generated stress wave, based on which the energy transfer is evaluated.

#### 3 MEASUREMENT OF SPT ENERGY TRANSFER RATIO

#### 3.1 The site and tests performed

The test site is located at a reclaimed area in Hong Kong. The interpreted ground profile and the locations where the SPT energy measurements were conducted are shown in Figure 2. This site generally comprises sandy FILL with rock fragments overlying sandy or silty ALLUVIUM before reaching Completely Decomposed Granites (CDG) above the bedrock. The SPT Analyzer was used to measure the ETR of six SPTs in a borehole covering soils with contrasting penetration resistance (*N*-value ranging from 17 to > 100) at about 24 m to 62 m below the ground level. All tests were performed by the same operator using the same SPT equipment and drill rig.

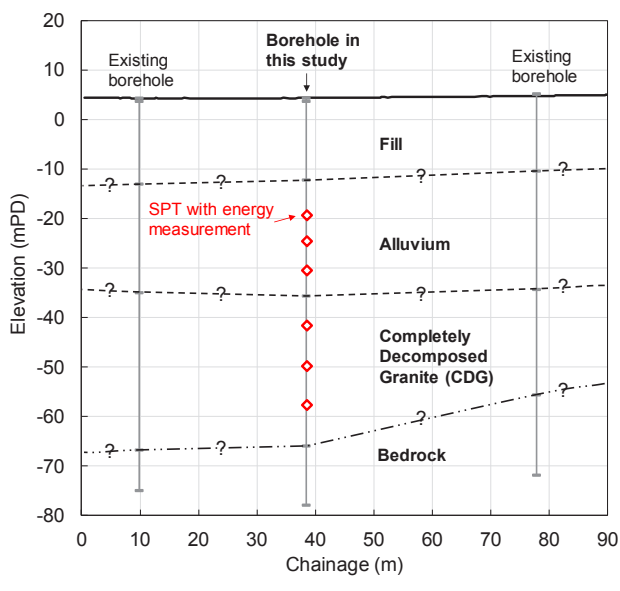


Figure 2. Interpreted ground profile of the test site and locations of SPT energy measurement.

#### 3.2 Measured energy transfer ratios

The energy E(t) transferred to the drill rod assembly was calculated using the Force Velocity (FV) method, which is considered fundamentally correct (Abou-mater & Goble 1997) and is adopted as the standard procedure for SPT energy calculation (ASTM 2016). In this method, E(t) is obtained by integrating the measured time-histories of force F(t) and velocity v(t) measured by the SPT Analyzer using Eq. 2.

$$E(t) = \int F(t)v(t)dt \tag{2}$$

The ETR is defined as the maximum of E(t) divided by the theoretical potential energy of the hammer drop (470.92 J for this SPT equipment).

A total of 554 data of valid energy measurements were obtained. As the rod lengths for all tests were larger than 10 m, no rod length correction was applied (Youd *et al.* 2001). Figure 3 shows the frequency distribution of the measured ETR. The data demonstrate a normally distributed relationship with a mean ETR of 66.1% (standard deviation = 5.6%; coefficient of variation = 8.5%). The results are within the typical range of ETR of the automatic trip hammer reported by others (e.g. Batilas *et al* 2016).

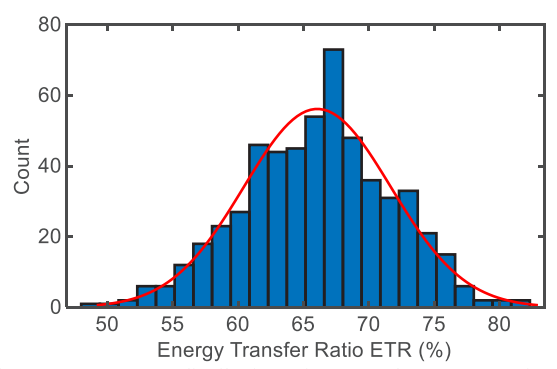


Figure 3. Frequency distribution of measured energy transfer ratios (ETRs).

Figure 4 plots the mean ETR  $\pm$  one standard deviation obtained for each SPT over the soil depth. The measured SPT *N*-values are also shown. As may be observed, the ETR measured in alluvial silt/sand, which the average *N*-value is relatively low (about 30), is generally lower than those measured in CDG, which the average N-value is much higher (> 100). In fact, Bosscher and Shower (1987) suggested that hard soils would result in higher energy transfer than soft soils.

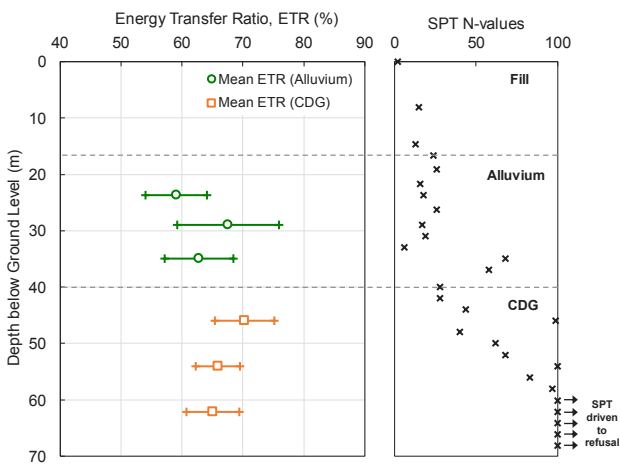
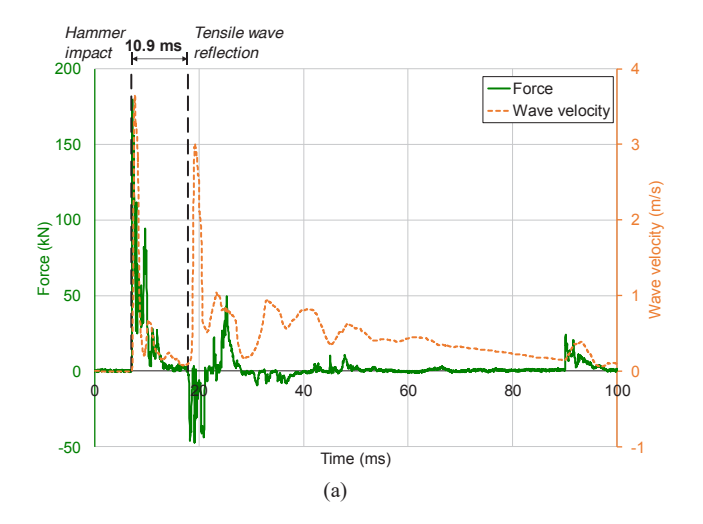


Figure 4. Energy transfer ratios versus depth, and SPT N-value profiles.

# 4 EFFECT OF SOIL PENETRATION RESISTANCE ON STRESS WAVE PROPAGATION

From the above, it is noted that the soil penetration resistance could have an effect on the ETR. In this Section, this effect is examined from the perspective of stress wave propagation based on a study of the force- and velocity-time histories measured by the SPT Analyzer.

In general, two distinctive types of stress wave propagation characteristics, featuring a tensile wave reflection in a hammer blow with low penetration resistance (Figure 5) and a compression wave reflection in a blow with high penetration resistance (Figure 6), can be observed. These phenomena are accompanied by different modes of hammer-anvil interaction based on the high-speed camera image analysis using the particle image velocimetry (PIV) method. The results are discussed as follows.



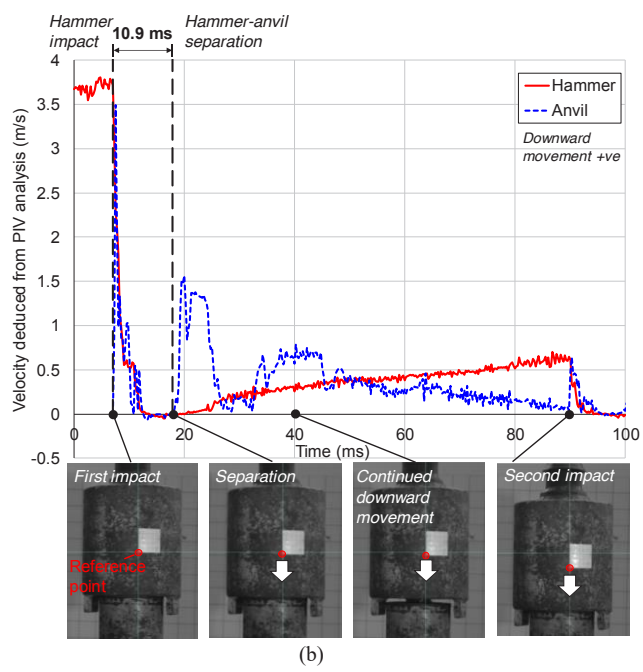
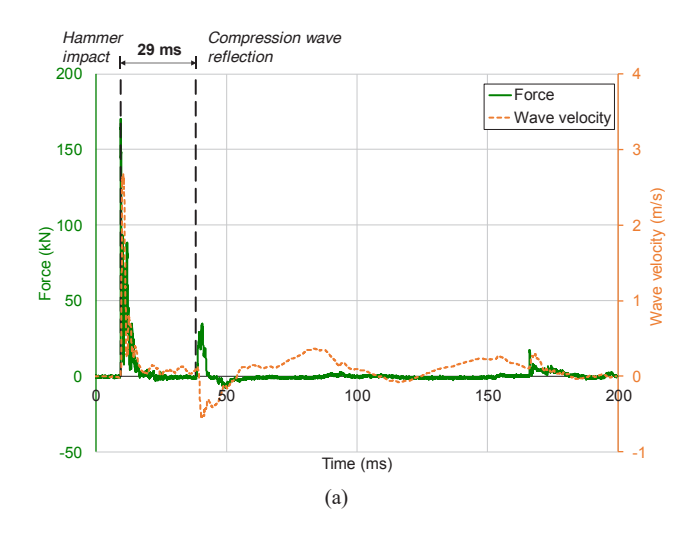


Figure 5. Hammer blow with low penetration resistance (23.7 mbgl, N = 18): (a) Force- and velocity-time histories of stress wave propagation measured by the SPT Analyzer; and (b) Travel velocities of hammer and anvil deduced from PIV analysis of high-speed camera footages.



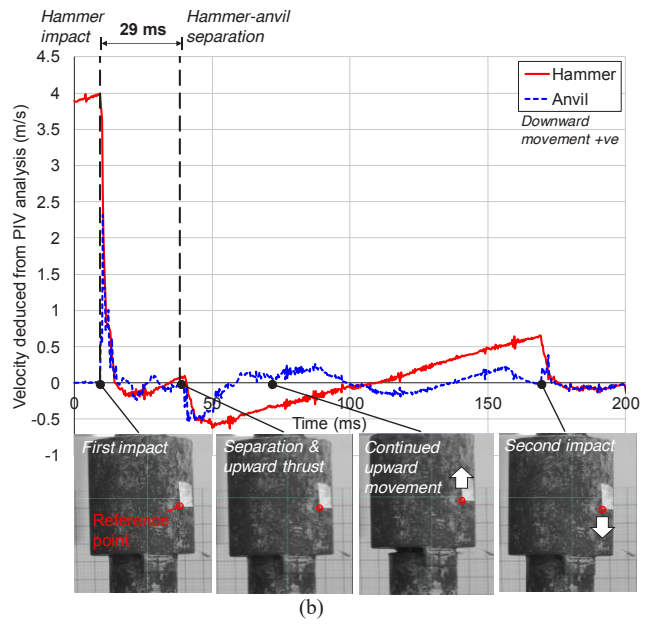


Figure 6. Hammer blow with high penetration resistance (62.1 mbgl, N > 100): (a) Force- and velocity-time histories of stress wave propagation measured by the SPT Analyzer; and (b) Travel velocities of hammer and anvil deduced from PIV analysis of high-speed camera footages.

# 4.1 Tensile wave reflection in hammer blow with low penetration resistance

Figure 5(a) shows the force and velocity measurements for a blow in alluvial sand (23.7 mbgl, N=18). This case is characterised by the low penetration resistance of the soil. When a compression wave generated by the hammer impact travels down to the tip of the drill rod assembly, a tensile wave is reflected because of the nearly free end condition, which means the soil impedance is less than the rod impedance. The tensile wave returns to the top of the rod and triggers a hammeranvil separation. The cut-off time is essentially the time when the force changes direction (from compression to tension), i.e. about 11 ms after impact in this case. Subsequently, the wave reflection and propagation continue but at a much reduced amplitude.

# 4.2 Compression wave reflection in hammer blow with high penetration resistance

Figure 6 shows the results for a high penetration resistance blow in CDG (62.1 mbgl, N > 100, driven to refusal). As observed in the stress wave measurement, a compression wave was detected at about 29 ms after impact, indicated by the second peak in the force-time history. This cut-off time again corresponds well with the hammer-anvil separation observed using the high-speed camera. A clear difference from the previous case is that the hammer is subjected to an upward thrust because of the reflected compression wave. These observations are typical of hammer blows with high penetration resistance.

The above observations are consistent with the fundamental theory of one-dimensional wave propagation, which suggests that a compression wave is reflected as a tension wave from a free-end but as a compression wave from a fixed-end. Soils with a low penetration resistance are akin to the free-end condition whereas soils with a high penetration resistance are akin to the fixed-end condition. It is worth noting that the latter condition is found to result in a higher energy transfer efficiency of SPT, as revealed in Section 3.

### 5 ENERGY LOSS IN THE HAMMER RELEASE PROCESS

Based on the energy measurement results discussed in Section 4, it is known that an average of about 34% of the hammer potential energy was dissipated before being delivered into the drill rod assembly. The potential sources of energy loss could be (1) frictional loss between hammer and guide rod during the hammer drop, (2) dissipation as heat and sound during the impact, (3) energy loss at the anvil (primarily dependent on anvil weight), and (4) strain energy in the guide rod due to bending in case of non-vertical impact, etc.

Amongst others, the first source of energy loss due to hammer-rod friction mentioned above can be realistically quantified by suitable physical measurement. For example, Kovacs (1979) measured the hammer impact velocity using light beam sensors, and calculated the hammer's kinetic energy before impact. Based on the test results, he recorded minimal energy loss for a mechanical free-fall hammer. On the other hand, Kovacs & Salomone (1982) found significant energy loss for the donut and safety hammers. For the automatic trip hammer employed in this study, there was, however, no such data available. Therefore, by using the high-speed camera, it is attempted to quantify the frictional energy loss during the hammer release process.

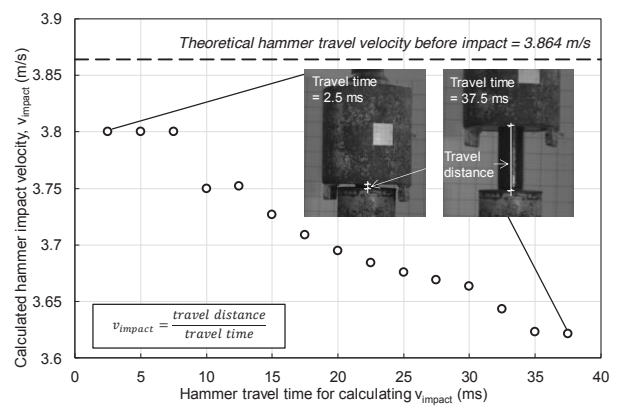


Figure 7. Typical results of calculated hammer impact velocity based on high-speed camera footages.

A total of eight hammer blows were recorded by the highspeed camera. In deriving the hammer impact velocity ( $v_{impact}$ ), the footages were analysed to track the movement of a reference point on the graph paper of the hammer. The hammer kinetic energy before impact is then calculated. The frictional energy loss is thus equal to the difference between the theoretical potential energy of the hammer fall and the calculated average kinetic energy before impact. With the highspeed camera, it is theoretically possible to determine the impact velocity even at 0.25 ms (i.e. one frame for a 4000 fps recording) before impact. However, considering the error in distance measurement involved, the calculation has been based on a ten-frame interval i.e. 2.5 ms lapsing a total of 150 frames i.e. 3.75 ms before impact. Figure 7 shows a typical result of the calculated impact velocity plotted against the time before impact for a hammer blow, including snapshots at two instants. The average  $v_{impact}$  of this plot is then used to calculate the kinetic energy before impact. The results are summarised in Table 1. It is found that the frictional energy loss ranges from about 4.3% to 11.3% of the theoretical potential energy, with an average value of 7.1%. In general, it means that 27% of the energy was lost due to other sources discussed above.

Table 1. Summary of calculated frictional loss during the hammer impact process.

Depth (mbgl)	Blow No.	Average $v_{impact}$ (m/s)	Kinetic energy before impact (J)	Frictional loss / Theoretical potential energy
23.7	1	3.71	434.1	7.8%
23.7	2	3.64	417.9	11.3%
23.7	3	3.72	436.5	7.3%
23.7	4	3.72	436.5	7.3%
34.9	86	3.78	450.7	4.3%
34.9	87	3.72	436.5	7.3%
62.1	53	3.75	443.5	5.8%
62.1	54	3.75	443.5	5.8%

# 6 CONCLUSIONS

This paper investigates the energy transfer characteristics of SPT based on high-speed camera footages of the hammer impact process and instrumentation monitoring of the stress wave propagation along the drill rod assembly. Key findings of this study are summarised in the following.

- The average energy transfer ratio of SPT using an automatic trip hammer measured at a reclamation site in Hong Kong is 66.1%. The energy efficiency is slightly higher at a greater depth (up to 62 m below ground level), where the soil penetration resistance is higher.
- Two distinctive types of stress wave propagation characteristics can be observed: tensile wave reflection in hammer blows with low penetration resistance and compression wave reflection in blows with high penetration resistance. These phenomena are evidenced by the direction of forces and wave velocity measured in the drill rod and the relative motion between the hammer and anvil.
- The energy loss during the automatic trip hammer release process has been quantified and is found to be about 7.1% based on image analysis of high-speed camera footages.

## 7 ACKNOWLEDGEMENTS

This paper is published with the permission of the Head of the

Geotechnical Engineering Office and the Director of Civil Engineering and Development, the Government of the Hong Kong Special Administrative Region, China.

#### 8 REFERENCES

Abou-Matar H. and Goble G.G. 1997. SPT dynamic analysis and measurements. J. Geotech. Geoenviron. Eng. 123 (10), 921-928.

Andrus R.D. and Stokoe K.H. 2000. Liquefaction resistance of soils from shear-wave velocity. *J. Geotech. Geoenviron. Eng.* ASCE 126 (11), 1015-1025.

ASTM 2016. Standard Test Method for Energy Measurement for Dynamic Penetrometers (ASTM D4633-16). ASTM International, West Conshohocken, PA.

Batilas A.V., Pelekis P.C., Roussos P.G., Athanasopoulos G. 2016. SPT energy measurements: manual vs automatic hammer release. *Geotech. & Geol. Eng.* ASCE 35 (2), 10 p.

Bosscher P. and Showers D. 1987. Effect of soil type on standard penetration test input energy. *J. Geotech. Eng.* ASCE 113 (4), 385-389

Brown D. 2009. Tracker video analysis and modelling tool. Open source, physics, 4.

HKSARG 2006. General Specification for Civil Engineering Works, 2006 Edition, Volume 1 of 2. The Government of the Hong Kong Special Administrative Region, 478 p.

Howie J.A., Daniel C.R., Jackson R.S. and Walker B. 2003.

Comparison of energy measurement methods in the standard penetration test. Report prepared for the U.S. Bureau of Reclamation, Geotechnical Research Group, Department of Civil Engineering, The University of British Columbia, Vancouver, Canada, 391 p.

ISO 2005. Geotechnical Investigation and Testing – Field Testing. Part 3: Standard Penetration Test (BS EN ISO 22476-3:2005). British Standards Institution, 24 p.

Kovacs W.D. 1979. Velocity measurement of free-fall SPT hammer. *J. Geotech. Eng.* ASCE 105 (1), 1-10.

Kovacs W.D. and Salomone L.A. 1982. SPT hammer energy measurement. *J. Geotech. Eng.* ASCE 108 (GT4), 599-620.

Kwong J.S.M. 1997. Interim review of the Standard Penetration Test procedures with reference to Hong Kong Practice (TN 2/97). Geotechnical Engineering Office, Hong Kong, 32 p.

PDI 2015. Manual for the SPT Analyzer System. Pile Dynamics Inc.,

Schmertmann J.H. and Palacios A. 1979. Energy dynamics of SPT. *J. Geotech. Eng.* ASCE 105 (8), 909-926.

Seed H.B., Tokimatsu K., Harder L.F. and Chung R.M. 1985. The influence of SPT procedures in soil liquefaction resistance evaluations. *J. Geotech. Eng.* ASCE 111 (12), 1425-1445.

Skempton A.W. 1986. Standard penetration test procedures and the efforts in sands of overburden pressure, relative density, particle size, ageing and overconsolidation. *Géotechnique* 36 (3), 425-447.

Stroud 1988. The Standard Penetration Test - Its application and interpretation. *Geotechnology Conference on Penetration Testing*, ICE, UK, 21 p.

Terzaghi K. and Peck R.B. 1967. Soil Mechanics in Engineering Practice (Second edition). Wiley, New York, 729 p.

Thielicke W. and Stamhuis E.J. 2014. PIVlab – Towards user-friendly, affordable and accurate digital particle image velocimetry in MATLAB. *Journal of Open Research Software* 2 (1), e30, DOI: http://dx.doi.org/10.5334/jors.bl.

Yang W.W. 2006. Development and application of automatic monitoring system for standard penetration test in site investigation. PhD Thesis, The University of Hong Kong, 258 p.

Yang W.W., Yue Q.Z.Q., and Tham L.G. 2012. Automatic monitoring of inserting or retrieving SPT sampler in drillhole, *Geotechnical Testing Journal* 35 (3), 420-436.

Youd T.L., Idriss I.M., Andrus R.D., Arango I., Castro G., Christian J.T., Dobry R., Finn W.D.L., Harder Jr. L.F., Hynes M.E., Ishihara K., Koester J.P., Liao S.S.C., Marcuson III W.F., Martin G.R., Mitchell J.K., Moriwaki Y., Power M.S., Robertson P.K., Seed R.B., Stokoe II K.H. 2001. Liquefaction resistance of soils: summary report from the 1996 NCEER and 1998 NCEER/ NSF workshops on evaluation of liquefaction resistance of soils. J. Geotech. Geoenviron. Eng. ASCE 127 (10), 817-833.